AIP | Applied Physics Letters

Fabrication of free-standing ordered fluorescent polymer nanofibres by electrospinning

J. R. Y. Stevenson, S. Lattante, P. André, M. Anni, and G. A. Turnbull

Citation: Applied Physics Letters **106**, 173301 (2015); doi: 10.1063/1.4918660
View online: http://dx.doi.org/10.1063/1.4918660
View Table of Contents: http://scitation.aip.org/content/aip/journal/apl/106/17?ver=pdfcov
Published by the AIP Publishing

Fabrication of free-standing ordered fluorescent polymer nanofibres by electrospinning

J. R. Y. Stevenson,[1] S. Lattante,[2] P. André,[1,3] M. Anni,[2] and G. A. Turnbull[1]
[1]*Organic Semiconductor Centre, SUPA, School of Physics and Astronomy, University of St Andrews, St Andrews, Fife KY16 9SS, United Kingdom*
[2]*Dipartimento di Matematica e Fisica "Ennio de Giorgi," Università del Salento, Via per Arnesano 73100, Lecce, Italy*
[3]*RIKEN, Wako, Saitama 351-0198, Japan*

(Received 19 January 2015; accepted 28 March 2015; published online 28 April 2015)

We demonstrate a static fabrication approach to make free-standing ordered arrays of fluorescent nanofibres through control of the transverse electrospinning field. The alignment and the density of the nanofibre arrays are optimised by careful design of both the source and collector electrode geometries which can control the transverse electric field over the full path of the jet. In doing so, we fabricate suspended fluorescent nanofibres with an aspect ratio of 10^4, and with a substantially increased density and order parameter (by a factor of ~10 compared to random deposition). Electrostatic modelling suggests that the field distribution of the component is the main contribution to the ordering between the plates. This method offers increased efficiency for the creation of ordered fibres collected over a small area and the characterisation of their photoluminescent properties. © *2015 AIP Publishing LLC*. [http://dx.doi.org/10.1063/1.4918660]

Electrospinning is a versatile method for the production of polymer fibres with diameters ranging from nanometers to microns. Fibres produced in this manner have a wide range of applications, and, with the introduction of emissive materials, they are of particular interest as nanophotonic light sources.[1–3] The electrospinning process works by the formation of a charged jet of polymer solution which is accelerated towards a grounded plate where the fibres are collected. During transit, the solvent evaporates and dry fibres are collected on a substrate above the ground plate.[4–6] This process normally yields a randomly oriented mat of fibres due to the inherent instabilities in the path of the jet. Oriented fibres, however, can be produced by changing the collection geometry, and several configurations have been used, such as patterned electrodes for the collection plates,[7,8] rotating drums to collect the fibre in an extended manner,[9,10] and large scale changes to the geometry of the base plate.[11–13]

For some applications of nanophotonic emitters, it would be very attractive to fabricate freestanding ordered arrays, e.g., to make higher numerical aperture fluorescent optical concentrators[14] or to achieve maximum surface area for chemical/biological fluorescent sensors.[15] In this paper, we show that it is possible to make free-standing ordered arrays of fluorescent nanofibres in a static apparatus by careful control of the transverse electrospinning field. We optimise both the alignment and the density of the nanofibre arrays through optimisation of both the source and collector electrode geometries, which can control the transverse electric field over the full path of the jet. We extend the source electrode as a plate to give a more uniform electric field which leads to a more efficient collection process (by a factor of 9) through an enhanced focussing of the fibres onto the collector. A pair of parallel ground electrodes are used to break the symmetry of the collection electrode to achieve ordered fibres. In doing so, we fabricate suspended fluorescent nanofibres with an increased order parameter (by a factor of 10) and aspect ratio of 10^4.

Fluorescent nanofibers were made by electrospinning dye-doped polystyrene solutions. Polystyrene (PS, average Mn 230 kD) was obtained from Sigma Aldrich. Rhodamine B laser dye was obtained from Exciton. All solutions were made from mixed powders of PS and Rhodamine B (5% by weight of PS) which were co-dissolved in N, N–dimethyl formamide (DMF from Sigma Aldrich) at a range of PS concentrations (5% wt./vol. to 30% wt./vol. in 5% steps). This range of solutions was first used to deposit fibres (with the setup shown in Fig. 1(b)) to select an appropriate concentration for deposition of aligned fibres.

Fig. 1 shows schematics of the electrospinning apparatus used. Two adaptations have been made to the standard electrospinning apparatus (Fig. 1(a)) to achieve concentrated, aligned, and freestanding fibres. The first alteration is the addition of a top plate with the needle tip protruding around 1 cm through its surface (see Fig. 1(b)). The needle used was a flat nosed 18 gauge aluminium needle, and the top plate was made from brass, 10 cm × 10 cm × 1 cm with a 3 mm diameter hole in the middle to permit the needle to pass through. The second change is the alteration of the collection geometry. The single ground plate was replaced with two parallel vertically oriented ground plates (see Fig. 1(c)) or two parallel horizontal metal wires. Aluminium plates—of thickness 2 mm, mounted in a custom designed holder made of polytetrafluoroethylene (PTFE)—were used for these collection electrodes. With such a setup, the electrospinning process is changed at the ground plates, where the broken symmetry of the electric field between the two plates leads to the collection of oriented fibres suspended between the two plates. To deposit fibres, the solution was pumped at a rate of 1 ml/h by an Aladdin 1000 syringe pump. The voltage was applied with a Universal HV350R with a range from 0 to 30 kV.

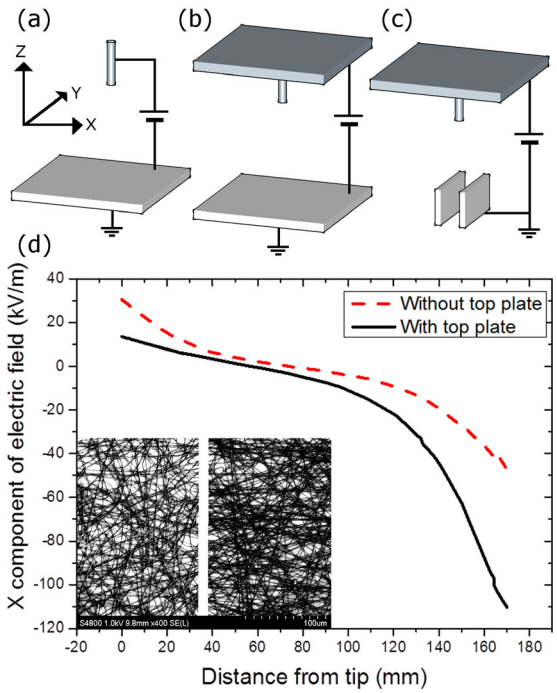

FIG. 1. Electrospinning setups used (a) standard configuration with a source needle and flat ground plate, (b) standard with the addition of a top plate, and (c) as in (b) but with the change of a single ground plate to parallel plates. (d) Calculated dependence of the *x*-component of the electric field at a point 40 mm in the positive *x* direction from the needle axis. The inset to (d) shows SEM images of collected fibres density without a top plate (left) and with a top plate (right), illustrating the increase in deposition density for the configuration in (b).

Each set of fibres was made from a common batch of solution, and samples were taken at three different voltages: 17, 20, and 26 kV. Initially, solution concentration and spinning voltage were optimised using the standard ground plate design (Fig. 1(b)) with the tip to collector distance fixed at 17 cm. Fibres were deposited on glass substrates and imaged with a scanning electron microscope (SEM). Nanofibres were deposited from solutions of concentrations 10% to 25% as detailed in the supplementary material.[16] Average fibre diameters varied from 290 ± 50 nm for 10% concentration at 17 kV to 1200 ± 200 nm for 25% concentration at 26 kV. We found that the introduction of the top plate has several consequences on the electrospinning process. The applied voltage required to initiate electrospinning increased by around 3 kV for equivalent samples, and led to a more concentrated deposition of fibres in a reduced area of only 5 cm^2, in comparison to a deposition area of around 45 cm^2 when using the standard configuration, Fig. 1(a). The corresponding increase in fibre density is shown in the two SEM images inset to Fig. 1(d). The left image shows the fibres deposited from a 15% concentration solution in the Fig. 1(a) configuration, and the right image shows the equivalent deposition with the configuration in Fig. 1(b). The increase in the voltage required for jet initiation is due to the uniform potential across the top plate, which reduces the force (the potential gradient) acting on the solution at the tip for equivalent voltages. The inclusion of the top plate has been suggested to control the whipping motion of the fibres and thus bring about a concentrating effect on the collected fibres on the ground plate.[17] To understand this effect better, modelling of the transverse electric field was undertaken using a finite element method in the COMSOL electrostatics module. Results of the modelling are shown in Fig. 1(d), which shows the x-component of the electric fields in configurations with and without a top plate. Each case shows a change from an outward transverse field to an inward field with increasing z-distance from the needle, but with some clear differences in the field magnitude. The axial regions where this is clearest are just below the tip and just above the collection area. Just below the tip, the addition of the top plate approximately halves the outward field. Conversely, immediately before the collection region, the configuration with a top plate shows a much stronger field. This means that the addition of a top plate causes the jet initially to be propelled from the axis less, and then brought back to the axis more strongly, resulting in an overall reduced spread of the deposition area. Further details of the change in transverse field with height are given in Fig. S1 in the supplementary material.[16]

To control the orientation of the fibres, the parallel plate collector was next assembled (Fig. 1(c)). Ordered fibres were produced with the same range of voltages as used for the random fibres and with a range of plate separations (0.7 cm, 1.0 cm, 2.0 cm, 4.0 cm). The tip to collector distance (17 cm) was measured from the inner top edge of the parallel plates.

The aligned fibres, suspended between the plates, were harvested initially on cut microscope slides by lifting the slide up between the plates, and images were recorded with an SEM (Fig. 2). Suspended fibres were also collected between two parallel wires on a custom substrate for a 0.7 cm collector separation. As with the random case, the fibres were sized from the SEM images. We observed that the plate separation appeared to have no systematic effect on the fibre diameter but the aligned fibres did show an increase in diameter with voltage. For a plate separation of 1 cm, the diameters increased from 440 ± 50 nm at 17 kV to 690 ± 130 nm at 26 kV. A full set of the diameter measurements are included in Table S2 in the supplementary material.[16]

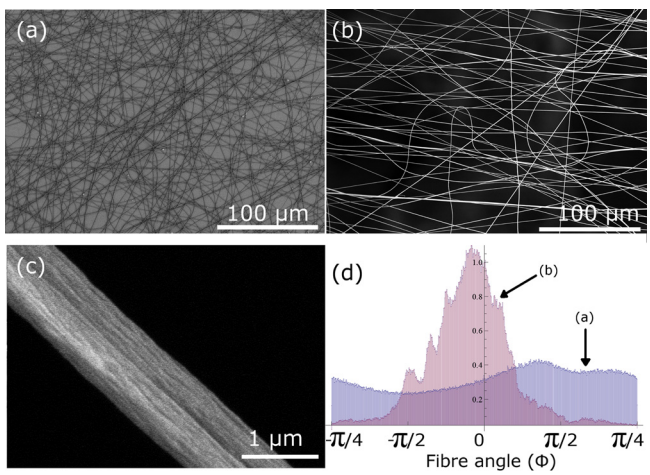

FIG. 2. (a)–(c) SEM images of fibres deposited from a 15% solution with an applied voltage of 20 kV, (a) random orientation; (b) and (c) suspended aligned fibres with a plate separation of 0.7 cm for scale bars of (a) and (b) 100 μm and (c) 1 μm. (d) Histograms of the distribution of fibre orientations within images (a) and (b), showing, respectively, their wide and narrow distributions.

To quantify the degree of ordering of the fibres, the following order parameter was used:

$$g_p = \frac{8}{5}\left\{\int_{-\pi/2}^{\pi/2} \cos^4(\Phi)\,\Psi(\Phi)d\Phi - 3\right\}, \quad (1)$$

where the fibre orientation function, $\Psi(\Phi)$, is the probability of finding a fibre at an angle Φ to the overall direction of alignment. In a sample where all fibres are perfectly aligned, $g_p = 1$, whereas in a completely random sample with no preferred orientation, $g_p = 0$.[11,18] For each SEM image, the fibre edges were identified and then g_p was calculated using a code written in Mathematica.

Fig. 3 shows the order parameter, g_p, for both aligned and random nanofibres. There is a large difference in the level of order between standard deposition (Figs. 1(b) and 2(a)) and the dual plate collection (Figs. 1(c) and 2(b)) as illustrated on Fig. 2(d). The data for 15% solution concentration are shown here for comparison with the ordered fibres, and fibres from other concentrations are given in Table S3 in the supplementary material.[16] In random samples, the order parameter was low, between 0.02 and 0.05. In comparison, the aligned samples collected with the parallel plates have relatively high values, typically closer to 0.3. In aligned samples, it can be observed that a much higher degree of ordering was obtained with the highest values of g_p observed for the 0.7 cm separation, suggesting that the narrower gaps allow for more ordered collection of fibres. Further to this, the data obtained directly on suspended fibres exhibit an enhanced order parameter of 0.52. This suggests that the transfer process to the substrate (lifting through the suspended fibres) potentially reduces the order of the fibres. While these order parameter values are lower than reported in other studies,[11,13] we note that our orientation measurement is carried out on a sample of higher fibre density, takes into account all fibres, and does not selectively discount any outliers.

To better understand the effect of gap length on the alignment process, the transverse electric field was modelled using COMSOL. Figs. 4(a) and 4(b) show the transverse x-component of the electric field, E_x, normal to the plates for two different separations; positive values correspond to fields pointing to the right and negative values to the left. We find that, as the plates are moved apart, the electric field close to each electrode changes little in either the magnitude or distribution. However, the region in the middle of the gap, in which E_x is close to zero and therefore similar to E_y, grows with increasing gap distances.

The z-component (downward) of the electric field was also calculated. Figs. 4(c) and 4(d) show two main changes in the field for the different plate separations. For small gaps, the z field-component is strong across the whole gap (rather than being concentrated in two distinct regions), and this strong region extends higher towards the tip. So for small gaps, the enhanced z-field tends to pull the charged fibre over the gap, rather than to an individual electrode. When one region of the fibre contacts an electrode, it will locally discharge, reducing the force on the fibre close to that electrode. Adjacent sections of the fibre will then tend to align

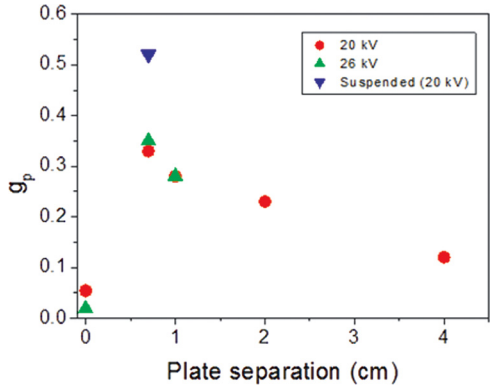

FIG. 3. Order parameters calculated as a function of plate separation and voltage for an experimental setup as in Fig. 1(c). Zero plate separation is represented by the flat collector plate (Fig. 1(b)).

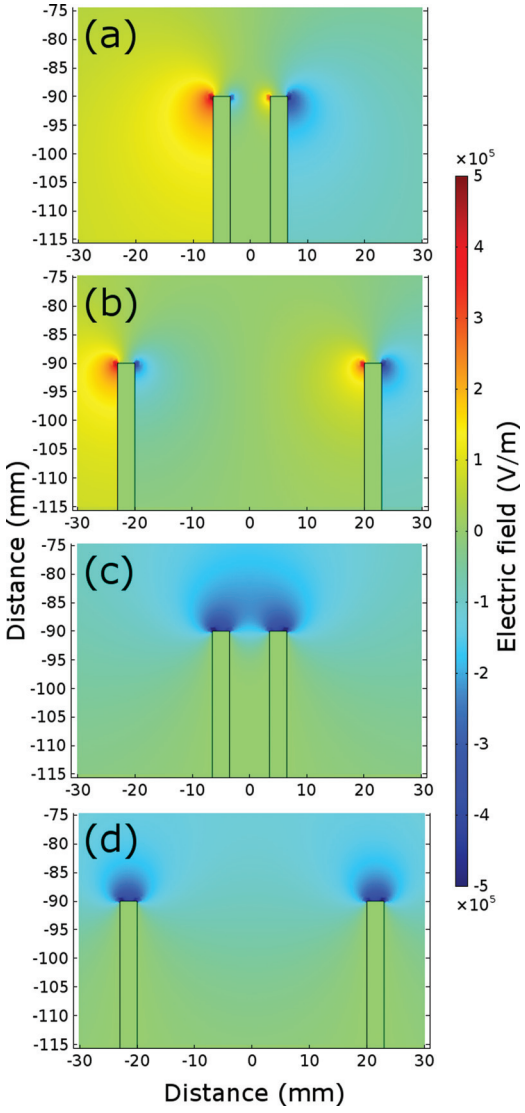

FIG. 4. (a) and (b) x-component (horizontal) and (c) and (d) *z*-component (vertical) of the electric field in the *x-z* plane around the parallel collection plates (shown in outline) for (a) and (c) 0.7 cm separation and (b) and (d) 4 cm separation. Red represents the strongest positive *x*-component. Field plots for all separations are given in Figs. S2 and S3 in the supplementary material.[16]

with the local electric field across the gap. As mentioned previously, when the gap is reduced, the x-field component dominates the (near-zero) y-component over most of the gap, and so the fibres will tend to align perpendicular to the electrodes. For wider gaps, the transverse field is similarly aligned but with reduced contrast between x- and y-field components across much of the gap.

The photophysical properties of the fibres were also examined (see supplementary material,[16] Fig. S4). Photoluminescence (PL) and photoluminescence excitation measurements of suspended fibres, prepared with 5% dye loading, were examined. It was not possible to measure the fibre absorption directly due to the relatively low concentration and the scattering nature of the mats of fibres. Fluorescence images of the fibres were recorded using an inverted Nikon Eclipse C1 scanning confocal microscope which confirmed that the dye was evenly distributed along the fibre. We found that the fibres showed no preferential polarisation of the PL, indicating that the dipoles of the dye molecules are randomly oriented within the PS matrix.

In summary, we have demonstrated a static electrospinning method for the production of suspended, ordered fluorescent fibres, with the use of custom source and collector electrodes that control the transverse electrospinning field. Fibres with diameters from around 500 nm to 700 nm have been made with an ordered orientation and an aspect ratio of 10^4. The aligned fibres have an order parameter up to 10 times that of random fibres deposited under comparable conditions, with the free-standing suspended fibres exhibiting the greatest alignment. The Rhodamine-B doped fibres show uniform, unpolarised fluorescence along their length.

We are grateful to the Engineering and physical Sciences research Council for financial support. We thank Dr Michael Mazilu for helpful discussions about data processing.

[1]A. Camposeo, F. Di Benedetto, R. Stabile, A. A. Neves, R. Cingolani, and D. Pisignano, Small **5**, 562 (2009).
[2]F. Gu, H. Yu, P. Wang, Z. Yang, and L. Tong, ACS Nano **4**, 5332 (2010).
[3]G. Morello, A. Polini, S. Girardo, A. Camposeo, and D. Pisignano, Appl. Phys. Lett. **102**, 211911 (2013).
[4]D. H. Reneker, A. L. Yarin, E. Zussman, and H. Xu, Adv. Appl. Mech. **41**, 43 (2007).
[5]A. Greiner and J. H. Wendorff, *Self-Assembled Nanomaterials I- Nanofibers*, edited by T. Shimizu (Springer, Berlin Heidelberg, 2008), pp. 107–171.
[6]P. Raghavan, D. H. Lim, J. H. Ahn, C. Nah, D. C. Sherrington, H. S. Ryu, and H. J. Ahn, React. Funct. Polym. **72**, 915 (2012).
[7]D. Li, Y. L. Wang, and Y. N. Xia, Adv. Mater. **16**, 361 (2004).
[8]Q. Z. Yu, M. Wang, and H. Z. Chen, Mater. Lett. **64**, 428 (2010).
[9]P. Katta, M. Alessandro, R. D. Ramsier, and G. G. Chase, Nano Lett. **4**, 2215 (2004).
[10]M. J. Laudenslager and W. M. Sigmund, J. Nanopart. Res. **15**, 1487 (2013).
[11]S. H. Park and D. Y. Yang, J. Appl. Polym. Sci. **120**, 1800 (2011).
[12]H. Yan, L. Q. Liu, and Z. Zhang, Appl. Phys. Lett. **95**, 143114 (2009).
[13]X. F. Wang, H. B. Zhao, L. S. Turng, and Q. Li, Ind. Eng. Chem. Res. **52**, 4939 (2013).
[14]N. C. Giebink, G. P. Wiederrecht, and M. R. Wasielewski, Nat. Photonics **5**, 694 (2011).
[15]X. Y. Wang, C. Drew, S. H. Lee, K. J. Senecal, J. Kumar, and L. A. Sarnuelson, Nano Lett. **2**, 1273 (2002).
[16]See supplementary material at http://dx.doi.org/10.1063/1.4918660 for further details of nanofibre deposition parameters, and photophysical properties of the nanofibres. In Tables S1 and S2, we list the measured diameters of random and aligned fibers. Table S3 lists the calculated order parameters of the fibers. In supplementary Figure S1, we show the x-component of the transverse electric field, at a range of distances below the tip. Figures S2 and S3 show the x- and z-electric field components close to the parallel collection plates. Figure S4 shows a fluorescence image of the fibres and their photoluminescence excitation and emission spectra.
[17]P. Kiselev and J. Rosell-Llompart, J. Appl. Polym. Sci. **125**, 2433 (2012).
[18]F. Gadalamaria and F. Parsi, Polym. Compos. **14**, 126 (1993).